Phase Behavior of Diblock Copolymers between Styrene and *n*-Alkyl Methacrylates

A.-V. G. Ruzette, P. Banerjee, and A. M. Mayes*

Department of Materials Science and Engineering, Massachusetts Institute of Technology, Cambridge, Massachusetts 02139

M. Pollard and T. P. Russell*

Polymer Science and Engineering Department, University of Massachusetts, Amherst, Massachusetts 01003

R. Jerome

Center for Education and Research on Macromolecules, University of Liege, Sart-Tilman, 4000 Liege, Belgium

T. Slawecki

Cold Neutron Research Facility, National Institute of Standards and Technology, Gaithersburg, Maryland 20899

R. Hjelm

Los Alamos Neutron Science Center, Los Alamos National Laboratory, Los Alamos, New Mexico 84745

P. Thiyagarajan

Intense Pulsed Neutron Source, Argonne National Laboratory, Argonne, Illinois 60439

Received July 6, 1998; Revised Manuscript Received September 23, 1998

ABSTRACT: In contrast to most diblock copolymers which exhibit the classical upper critical ordering transition (UCOT), polystyrene-*b*-poly *n*-butyl methacrylate—PS-*b*-PBMA—has been shown to undergo ordering upon heating through a lower critical ordering transition (LCOT). Here we report the phase behavior of a family of diblock copolymers formed from styrene and a homologous series of *n*-alkyl methacrylates, as determined by combined dynamic rheological testing and small-angle neutron scattering (SANS). It is shown that the shortest side chain methacrylates, with the exception of methyl methacrylate, exhibit the LCOT, while for side chains longer than *n*-butyl, the copolymers exhibit the classical UCOT behavior. Combined group contribution/lattice fluid model calculations of the solubility parameter and specific volume of the corresponding homopolymers qualitatively support these observations. The same calculations were further employed to molecularly design LCOT behavior into a new diblock material consisting of styrene and a random copolymer of methyl and lauryl methacrylate, denoted PS-*b*-P(MMA-*r*-LMA). The success of this approach suggests a simple semiquantitative method for predicting and designing the phase behavior of weakly interacting polymer pairs.

Introduction

The tendency of diblock copolymers to undergo ordering or microphase separation upon cooling through an upper critical ordering transition (UCOT) has been extensively studied, both theoretically[1−3] and experimentally.[4−9] In a departure from this classical behavior, diblock copolymers of styrene and *n*-butyl methacrylate, denoted here as PS-*b*-PBMA, have been shown to undergo a transition from the disordered to the ordered state upon heating.[10,11] More recently, a diblock copolymer of styrene and vinyl methyl ether was shown to exhibit the same trend of decreasing compatibility with increasing temperature.[12] This lower critical ordering transition (LCOT) is analogous to the lower critical solution transition (LCST) observed in polymer blends and solutions. A straightforward thermodynamic analysis of such phase behavior shows that both the enthalpy and the entropy changes upon demixing of the block segments at elevated temperatures must be positive.[13] In other words, the LCOT, in contrast to the classical, enthalpically driven UCOT, results from an increase in entropy, or an increase in the number of configurations available to the system, at high temperatures in the ordered state compared to the disordered state. Empirically, this increase in entropy on demixing is accompanied by a positive change in volume, which explains the reported pressure dependence of this transition.[14−16] High pressures favor the denser segmentally mixed state, thereby raising the ordering temperature.

The effect of pressure on the LCOT has important implications from an engineering standpoint. Small-angle neutron scattering studies on PS-*b*-PBMA under hydrostatic pressure reveal that the LCOT can increase by as much as 147 °C/kbar.[16] Pressure has an equally profound effect on the rheological properties of this material, enhancing flow by forcing segmental miscibility. From a processing viewpoint, such "baroplastic" behavior could offer increased flexibility in controlling structure and properties, as both temperature and

* To whom correspondence should be addressed.

10.1021/ma981055c CCC: $15.00
Published on Web 11/07/1998

Table 1. Characteristics of Diblock Copolymers Used

copolymer	$10^3 M_n$	M_w/M_n	PS fraction (wt %)	remarks
30K PS-*b*-PLMA	30	1.03	47	
45K PS-*b*-PLMA	45	1.05	49.5	
19K PS_{d8}-*b*-PLMA	19	1.01	50 (theor)	
23K PS-*b*-POMA	23	1.06	55.8	
43K PS-*b*-POMA	43	1.03	50.7	
27K PS-*b*-POMA	~27		54.3	30/70 wt% mixture of 43K and 23K
27K PS-*b*-PHMA	27	1.01	49.0	
50K PS-*b*-PHMA	50	1.01	57.4	~5% homopolymer
110K PS-*b*-PPMA	110	1.3	41	
136K PS-*b*-PPMA	136	1.01	49.8	<5% homopolymer
50K PS-*b*-PEMA	50	1.02	49.2	~5% homopolymer
110K PS-*b*-PEMA	110	1.01	48.7	<5% homopolymer
80K PS-*b*-P(MMA-*r*-LMA)	80	1.01	50	26.5 wt% MMA, 23.5 wt% LMA

pressure might equally be used to affect the thermodynamic state.

The compressible nature of systems that exhibit phase separation upon heating has led to the development of several theoretical treatments aimed at predicting such transitions and understanding their molecular origin. Typically, equation of state effects are incorporated into the classic free energy balance of two component systems to account for compressibility and nonzero volume changes upon mixing. Different equations of state have been used in combination with the random phase approximation (RPA) to extract segmental exchange interaction energies $\Delta\epsilon = (\epsilon_{11} + \epsilon_{22} - 2\epsilon_{12})/2$ (or $\chi = z\Delta\epsilon/kT$, where z is the coordination number) from SANS data and predict phase diagrams for polymer blends[17,18] and diblock copolymers[19−21] known to exhibit the LCST/LCOT.

Typically, systems exhibiting entropically driven phase separation are categorized either as those with strong specific interactions (e.g., hydrogen bonding, strong dipole/dipole or electron donor/electron acceptor interactions) or as more weakly interacting systems with molecular packing differences. In both cases, the denser nature of the mixed state equates to a loss of molecular configurations compared to the phase separated state, which drives phase separation upon heating. For strongly interacting systems such as PMMA/PVDF,[22] PMMA/PEO,[23] and, to a lesser extent, PS/PVME,[24] the loss of configurations is due to preferred orientation of the interacting chemical groups. For weakly interacting systems, on the other hand, molecular packing differences lead to differences in free volume of the pure components that are reflected in their specific volumes and thermal expansion coefficients. These disparities result in a densification, or reduction in free volume, of the mixed state.[25] PS/PBMA is thought to fall into this latter category, as both upper and lower critical temperatures have been found for diblock copolymers[10] and low molecular weight blends[26] of this polymer pair. This observation precludes the possibility of an exothermic heat of mixing for this system.

To better understand the molecular origin of the LCOT in the case of PS-*b*-PBMA and perhaps identify new LCOT-type systems, we investigated the phase behavior of a family of diblock copolymers formed from styrene and a homologous series of *n*-alkyl methacrylates. For PS-*b*-PMMA, the classical UCOT phase behavior is well documented.[27,28] Considering the remarkably different phase behavior of PS-*b*-PBMA compared to this system, one might expect that lengthening the alkyl side chain of the methacrylate should enhance the tendency toward LCOT behavior in this family of materials, due to the increasing disparity in free volume between styrene and the methacrylate block. Herein it is shown, through combined dynamic rheological testing/small-angle neutron scattering, that the opposite trend is observed. Namely, the shortest side chain methacrylates, with the exception of methyl methacrylate, all exhibit the LCOT, while for side chains longer than *n*-butyl only the UCOT is observed. These results are qualitatively supported by combined group contribution/lattice fluid model calculations of the solubility parameter and specific volume as a function of temperature for each of the corresponding homopolymers. On the basis of these findings, a new styrene/*n*-alkyl methacrylate block copolymer was molecularly designed and synthesized, which also displays the LCOT.

Experimental Section

Compositionally symmetric diblock copolymers of styrene and various *n*-alkyl methacrylates, namely, ethyl (EMA), propyl (PMA), hexyl (HMA), octyl (OMA), and lauryl methacrylate (LMA), were synthesized anionically, using *sec*-butyllithium as the initiator. All monomers were purified prior to synthesis using two distillations. MMA and EMA (Aldrich), PMA, BMA, and HMA (Polyscience Inc.), and S (Aldrich) monomers were first dried and distilled over CaH_2 and subsequently stored under a nitogen atmosphere at −10 °C until needed. Prior to polymerization, the methacrylate monomers were titrated with a 25 wt % trioctylaluminum solution (Aldrich) in hexane until a yellowish-green color developed[29] and were then distilled a second time. For styrene, the second distillation step was carried out over fluorenyllithium. The *sec*-BuLi initiator (Aldrich, 1.3 M solution in cyclohexane) was used as received. The polymerization reaction was carried out under nitrogen in THF that had been refluxed over a freshly prepared sodium-benzophenone complex. The solvent, containing 10 mol excess dried LiCl with respect to the required initiator amount, was cooled to −78 °C and titrated using one or two drops of distilled styrene and a dropwise addition of *sec*-BuLi until a persistent yellow/orange color developed. The required amount of *sec*-BuLi initiator was then injected, followed by the purified styrene monomer. Polymerization of the first block was allowed to proceed for 30 min, after which diphenyl ethylene was added in proportion with the amount of initiator used. After 5 min, an aliquot of polystyrene was extracted and terminated with methanol for molecular weight determination. The second monomer was then injected and polymerization allowed to proceed for 2 h before the reaction was terminated with methanol. Compositions were determined using ^1H nuclear magnetic resonance (NMR). Molecular weights were measured by gel permeation chromatography (GPC) in methylene chloride using PS standards. The characteristics of the different materials used for this study are listed in Table 1. The molecular weights listed are based on the measured weight fraction and molecular weight of the styrene block. For some materials, a small fraction of PS homopolymer was present, as noted in the table.

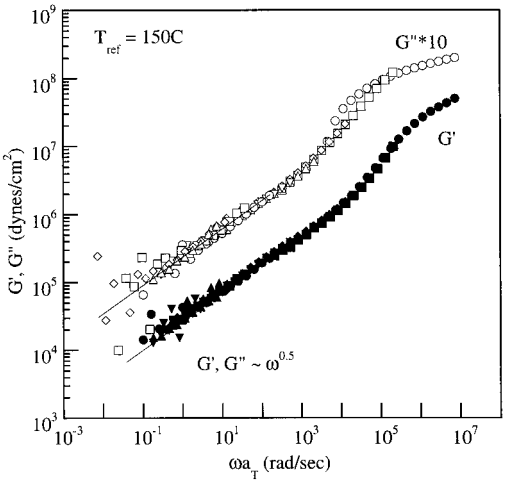

Figure 1. Master curves for the storage (G') and loss (G'') moduli of 45K PS-*b*-PLMA.

Dynamic rheological measurements were obtained using a Rheometric Scientific ARES rheometer operated in the parallel plate geometry, with 25 mm diameter plates and a 0.5 mm gap size. The dynamic storage (G') and loss (G'') moduli of the copolymers were determined isothermally as a function of frequency ($0.1 < \omega < 400$ rad/s), and temperature was varied from 100 to 200 °C in 10 °C increments. A strain of 0.5% was used, which is in the linear elastic regime for this family of materials. Whenever possible, the isothermal frequency sweeps obtained at various temperatures were superimposed about a reference temperature of 150 °C in order to obtain master plots. Data taken at torques lower than 1 g-cm (the lower limit of sensitivity of the transducer) were discarded. While dynamic rheological measurements offer a clear means of identifying whether a sample is ordered or disordered, they do not provide direct information on the type of phase diagram in hand (UCOT vs LCOT), unless a phase transition is observed in the temperature range studied. Therefore, this technique was used in combination with small-angle neutron scattering, the latter offering the advantage of revealing unambiguously whether composition fluctuations in the disordered state increase or decrease with increasing temperature, as expected for LCOT and UCOT behavior, respectively.

Small-angle neutron scattering measurements were obtained primarily at the Cold Neutron Research Facility at the National Institute of Standards and Technology on beamline NG-3. The instrument configuration was $\lambda = 6$ Å, $\Delta\lambda = 15\%$, and sample-to-detector distance = 6 m, resulting in a q range of 0.008−0.08 Å^{-1}. Some measurements were also taken at the Manuel Lujan Jr. Neutron Scattering Center of the Los Alamos Neutron Science Center at the Los Alamos National Laboratory on the Low-Q Diffractometer (LQD), and at the Intense Pulsed Neutron Source at the Argonne National Laboratory on the Small-Angle Neutron Diffractometer (SAND). The wavelength range and q range for these two time-of-flight diffractometers are $0.2 < \lambda < 20$ Å and $0.003 < q < 0.5$ Å^{-1} and then $1 < \lambda < 14$ Å and $0.0035 < q < 0.6$ Å^{-1}, respectively. In all cases, results were corrected for background and detector inhomogeneity in the standard manner and data were scaled to absolute units (cm^{-1}) using a silica standard. Temperature was varied by 10 or 20 °C increments, and sufficient time was provided for thermodynamic equilibration at each temperature. Thermodynamic reversibility of the observed behaviors was verified in each case through temperature cycling.

Results and Discussions

I. Copolymers with Long Alkyl Side Chain Methacrylates ($n \geq 6$). Figure 1 shows the storage (G') and the loss (G'') moduli of 45K PS-*b*-PLMA as a function of frequency at various temperatures, time/temperature superpositioned about a reference temperature of 150 °C. The results suggest that this material remains in the ordered state over the entire temperature range studied (100−190 °C), as is evident from the low-frequency power law behavior. Both G' and G'' scale with frequency approximately as $\omega^{0.5}$, which is typical for ordered diblock copolymers.[4,5] Similar results were obtained for the 30K sample. The persistence of the ordered state for temperatures a high as 200 °C is consistent with two distinctly different phase diagrams. One possibility is that the low temperature compatibility between styrene and the methacrylate strongly decreases with increasing alkyl side chain length. This would have the effect of raising the UCOT above the experimentally accessible temperature range, even for these rather low molecular weights. Alternatively, a simultaneous increase of the UCOT and decrease of the LCOT would result in an "hourglass" phase diagram in which the two transitions have essentially merged together such that the copolymer is ordered at all temperatures. To differentiate between these scenarios, SANS measurements were performed on these materials, as well as a lower molecular weight PS$_{d8}$-*b*-PLMA sample.

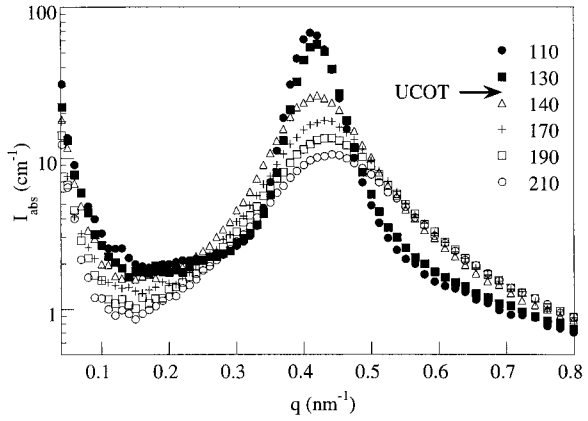

Figure 2. Scattering intensity profile for 19K PS$_{d8}$-*b*-PLMA.

Figure 2 shows the scattering intensity profile as a function of wave vector $q = 4\pi(\sin\theta)/\lambda$ for 19K PS$_{d8}$-*b*-PLMA. At temperatures below 130 °C, a Bragg reflection characteristic of the ordered state is observed at $q \approx 0.041$ Å^{-1}. Increasing the temperature above 130 °C results in a significant decrease in the peak intensity and a broadening of the scattering maximum. Such "correlation hole" scattering is a signature of the segmentally mixed state, indicating that this material undergoes a classic UCOT between 130 and 140 °C. Moreover, the magnitude of the thermodynamic fluctuations in the system or, equivalently, the intensity of the scattering maximum monotonically decreases with increasing temperature, thereby precluding the possibility of LCOT-type phase behavior for this sample in the temperature range probed (110−210 °C). The shift in peak position q^* toward higher q values as temperature increases supports the picture of a progressive relaxation of the coils as the system moves away from the ordering transition. For the 30K and 45K samples, sharp reflections were observed at all temperatures, confirming the ordered state apparent from the dynamic rheological measurements. A monotonic decrease in intensity of the first-order reflection with increasing temperature was also found, again ruling out LCOT behavior.

Similar results were obtained for PS-*b*-POMA and PS-*b*-PHMA, but with a distinct increase in block compat-

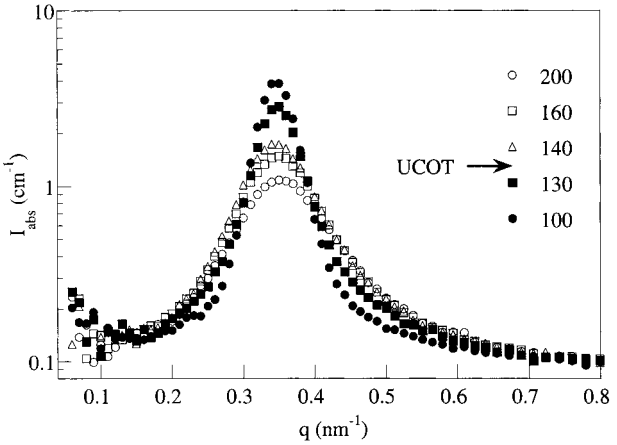

Figure 3. Scattering intensity profile for 27K PS-*b*-POMA.

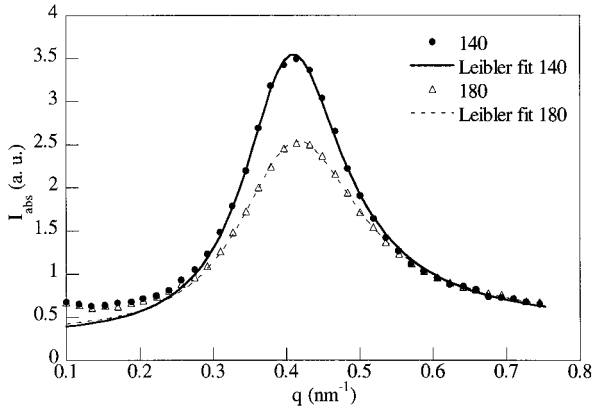

Figure 4. Scattering intensity profile for 23K PS-*b*-POMA at 140 °C and 180 °C and the corresponding Leibler fits.

ibility in going from lauryl to hexyl methacrylate. For PS-*b*-POMA, the 23K sample was disordered throughout the experimental temperature range while the 43K was ordered. As shown in Figure 3, a UCOT could be observed between 130 and 140 °C for a ~27K mixture of these two samples containing 70 wt % of the low molecular weight copolymer and prepared as described in ref 11. The use of mixtures has proven to be very successful in accessing transition temperatures without requiring further synthesis. Clearly, the bimodal nature of such mixtures affects the sharpness of the transition. However, estimates of the transition temperature for the monomodal sample of equivalent molecular weight can still be obtained, provided the two molecular weights used in the mixture are not too disparate.[6,11]

For PS-*b*-PHMA, both the 27K and 50K samples were disordered over the entire experimental temperature range. Nevertheless, the classical UCOT trend is also found; namely, the correlation hole scattering intensity monotonically decreases with increasing temperature.

To extract estimates of χ as function of temperature from the SANS data for these three UCOT-type systems, the well-known Leibler formalism[1] was employed

$$I(q) = \frac{(b_{PS} - b_{MA})^2}{v_{ref}} S(q) \qquad (1)$$

where

$$S(q) = \frac{N}{F(q) - 2\chi N} \qquad (2)$$

and b_i is the scattering length of component i, v_{ref} the reference volume of a segment, and N the number of statistical segments, equated here to the degree of polymerization of the molecule. For $F(q)$, the expression developed in the case of unequal statistical segment lengths for the two segment types and given by eqs A2−A4 in the appendix of ref 7 was used. Neutron scattering data were fit to eq 1 with χ, the statistical segment length of the methacrylate block a_{MA}, and a constant scaling factor as fitting parameters. A statistical segment length of 6.7 Å was used for PS.[27] Data for the lowest molecular weight samples were used in all three cases, i.e., 19K PS_{d8}-*b*-PLMA, 23K PS-*b*-POMA, and 27K PS-*b*-PHMA. Data were fit over temperature ranges in which the inverse peak intensity varied linearly with inverse absolute temperature. For PS-*b*-POMA and PS-*b*-PHMA, no suitable fit could be obtained without prior subtraction of an incoherent scattering background due to the high hydrogen content. As a first approximation, a constant background was included as a fitting parameter. An example of the resulting fit is given in Figure 4 for PS-*b*-POMA. The average values of the fitting parameters are listed in Table 2 along with the fitting temperature range and N for each material.

The interaction parameters are shown in Figure 5 where the functional form $\chi = A + B/T$ was used, with best fit slope and intercept values as listed. Data obtained by Sthün[28] for 27K PS-*b*-PMMA are included for comparison. The χ values are found to increase from approximately 0.044 to 0.083 when the side chain length is increased from 6 to 12 hydrocarbons. All of these systems are characterized by a weak temperature dependence and a large "entropic" contribution to χ. Such behavior, similar to that previously reported for PS-*b*-PMMA,[27,28] strongly suggests that other factors, such as differences in packing, chain flexibility, and self-interaction energies of the pure components, play a dominant role in the phase behavior of these systems. Such effects have been studied by several authors, using both lattice-based[30−32] and off-lattice[33,34] calculations on polymer mixtures of dissimilar components. These calculations show that disparities in monomer structure, chain flexibility and van der Waals self-interaction energies contribute both entropic and enthalpic terms to the free energy of mixing that result in reduced compatibility.

II. Copolymers with Short Alkyl Side Chain Methacrylates ($n \leq 4$). Strikingly different results were obtained for diblock copolymers between styrene and methacrylates with shorter alkyl side chains. Master curves for G' and G'' obtained for 136K PS-*b*-PPMA are shown in Figure 6. The data indicate that this system is disordered at low temperatures and goes through a LCOT between 160 and 165 °C. The transition is evidenced by the change in scaling of G' in the low-frequency regime from $G' \sim \omega^{1.4}$, characteristic of a segmentally mixed system,[4] to $G'' \sim \omega^{0.5}$. In the vicinity of the transition, good overlap of the data for both G' and G'' cannot be obtained through horizontal temperature shifts. Such failure of time/temperature superposition is commonly observed for systems characterized by large concentration fluctuations prior to ordering.[5]

The tendency of this system to microphase separate upon heating is further evidenced by the neutron scattering data from 110K PS-*b*-PPMA shown in Figure

Table 2. SANS Data Fitting Parameters

sample	*T* range (°C)	*N*	averaged χ	a_{MA} (Å)	incoherent scattering I_{inc} (cm^{-1})	scaling factor
19K PS_{d8}-*b*-PLMA	150−210	122	0.083	15 ± 1		0.1 ± 0.05
23K PS-*b*-POMA	120−200	175	0.056	12.3 ± 0.4	0.35 ± 0.02	0.02
27K PS-*b*-PHMA	150−215	221	0.044	10.8 ± 0.5	0.065 ± 0.001	0.005 ± 0.0002

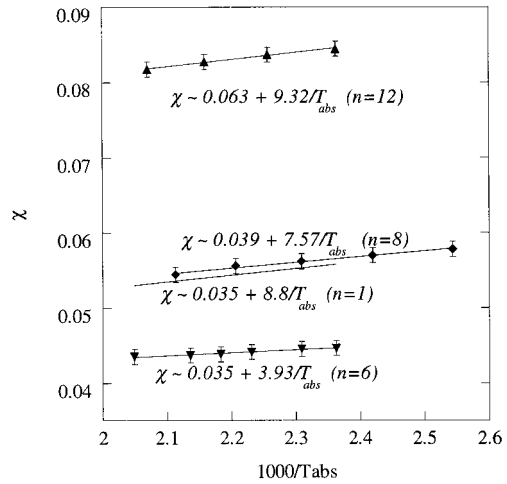

Figure 5. Segmental interaction parameters χ extracted from SANS data for 19K PS_{d8}-*b*-PLMA (*n* = no. of hydrocarbons in side chain = 12), 23K PS-*b*-POMA (*n* = 8) and 27K PS-*b*-PHMA (*n* = 6). Also shown is the interaction parameter for PS-*b*-PMMA (*n* = 1) listed in ref 28.

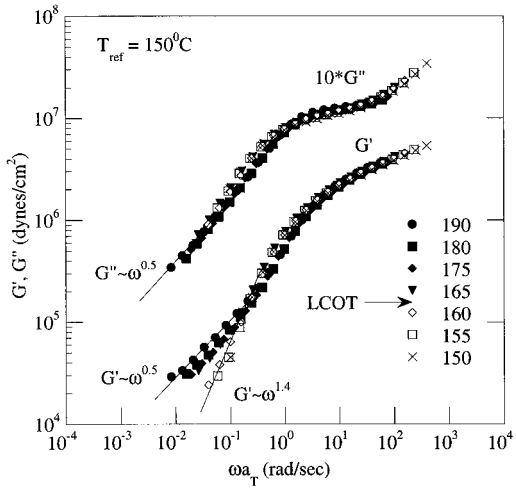

Figure 6. Master curves for the storage (*G′*) and loss (*G″*) moduli of 136K PS-*b*-PPMA.

7. The weak scattering maximum observed at low temperatures (T < 175 °C) increases in intensity as the LCOT is approached. Between 195 and 205 °C, the distinct narrowing of the scattering peak signals the onset of order. The weak scattering observed in the mixed state, far below the LCOT, witnesses a strong compatibility between styrene and propyl methacrylate compared with the styrene/*n*-alkyl methacrylate systems described in section I. This is evident upon comparing the disordered state (high temperature) scattering of, for example, PS-*b*-POMA (Figure 3), to that observed for PS-*b*-PPMA in the same state, i.e., at low temperatures (Figure 7). In fact, PS-*b*-PPMA appears to be more miscible than PS_{d8}-*b*-PBMA, since 75K PS_{d8}-*b*-PBMA orders around 200 °C while 110K PS_{d8}-*b*-PBMA is always ordered. While deuteration is generally known to affect miscibility, SANS experiments on hydrogenated PS-*b*-PBMA show that deuteration

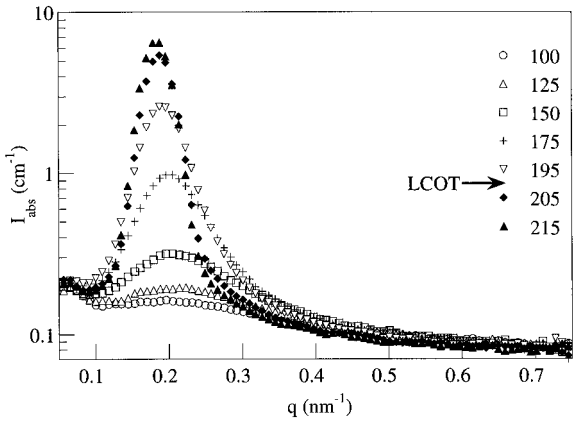

Figure 7. Scattering intensity profile for 110K PS-*b*-PPMA.

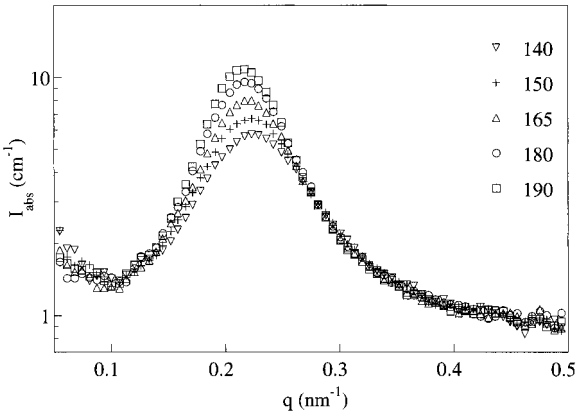

Figure 8. Scattering intensity profile for 50K PS-*b*-PEMA.

effects do not significantly alter the phase diagram for this system.[35]

Similar results were obtained for PS-*b*-PEMA. As shown in Figure 8, the intensity of the correlation hole scattering for 50K PS-*b*-PEMA continuously increases with temperature, although the LCOT is not observed between 140 and 190 °C. 110K PS-*b*-PEMA is, on the other hand, always ordered in this temperature range. Therefore PS-*b*-PEMA also displays LCOT-type behavior, although a lesser degree of compatibility is exhibited for this system compared to PS-*b*-PPMA. Earlier blend studies of PS/PEMA and PS/PPMA by Brannock and co-workers[36] seem to reveal the opposite, i.e., a higher degree of miscibility for PS/PEMA, although the use of melt indexes as molecular weight indicators in those studies complicates quantitative comparison with our observations.

III. Group Contribution Calculations. Table 3 summarizes the results presented in the two preceding sections, i.e, the type of behavior (UCOT vs LCOT) and transition temperatures for each system. Also included are the results reported for PS-*b*-PMMA[27,28] and PS-*b*-PBMA.[11] Although rigorous modeling of the complex phase behavior observed across this family of materials is beyond the scope of this paper, the following section presents some simple group contribution calculations which qualitatively support the experimental findings

Table 3. Summary of Phase Behavior and Transition Temperatures for Styrene/Alkyl Methacrylate Diblock Copolymers

copolymer	type of behavior	transition temperature
PS-*b*-PLMA	UCOT	30K, 45K: >200 °C
PS_{d8}-*b*-PLMA	UCOT	19K: 135 ± 5 °C
PS-*b*-POMA	UCOT	23K: <100 °C
		43K: >200 °C
		27K mixt.: 135 ± 5 °C
PS-*b*-PHMA	UCOT	27K: <100 °C
		50K: <100 °C
PS_{d8}-*b*-PBMA[a]	LCOT	75K: 200 ± 5 °C (LCOT)
	(+ UCOT)	85K: 165 °C ± 5 °C (LCOT)
		110K: ordered
PS-*b*-PPMA	LCOT	110K: 200 °C ± 5 °C
		136K: 162 ± 2 °C
PS-*b*-PEMA	LCOT	50K: >190 °C
		110K: ordered
PS_{d8}-*b*-PMMA[b]	UCOT	28K: <100 °C
PS-*b*-PMMA[c]	UCOT	27K: <100 °C

[a] Data from ref 11 and unpublished results. Only the LCOTs are given. [b] Data from ref 27. [c] Data from ref 28.

presented above. In the next section, we will further illustrate how such calculations might be successfully used to design-in the phase behavior of new systems.

A solubility parameter formalism relates the interaction parameter of a polymer pair to the solubility parameters of the individual components through the Hildebrand equation

$$\chi = \frac{v_1}{k_B T}(\delta_1 - \delta_2)^2 \tag{3}$$

where v_1 is the reference volume of polymer 1, k_B is the Boltzmann constant, T is the temperature, and δ_i is the solubility parameter of component i.[37] Although this formalism is known to have quantitative limitations, especially in the case of strongly polar systems, it is regularly used as an empirical scheme for predicting polymer miscibility. From eq 3, miscibility is expected when the solubility parameters of the individual components are very similar.

Solubility parameters for each homopolymer used in this study were calculated using group contribution methods, according to Van Krevelen.[38] The expression for δ includes contributions from dispersive forces (δ^d), dipole/dipole (δ^p) and hydrogen bonding (δ^H) interactions. The total solubility parameter δ is related to these three individual components by

$$\delta^2 = (\delta^d)^2 + (\delta^p)^2 + (\delta^H)^2 \tag{4}$$

Figure 9 shows δ for the *n*-alkyl methacrylate homopolymers as a function of the number of hydrocarbons n in the alkyl side chain, ranging from $n = 1$ (PMMA) to $n = 12$ (PLMA). The value of δ for the methacrylate monotonically decreases with increasing alkyl side chain length, which is consistent with the reported decrease in the glass transition temperature,[39] and indicates a progressive weakening of intersegmental interactions. Moreover, the value for polystyrene, which is indicated by the arrow, is found to lie closest to that of PBMA. This qualitatively supports the observation of a maximum in thermodynamic compatibility, or minimum in $\Delta\delta$, between the styrene and the methacrylate block for intermediate side chain lengths. For the particular formalism chosen here, the solubility parameter analysis predicts the maximum to occur around PBMA (see

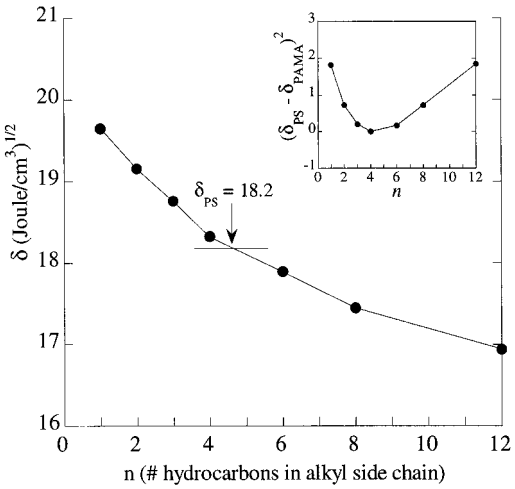

Figure 9. Calculated solubility parameters for poly *n*-alkyl methacrylates as a function of the no. of hydrocarbons n in the alkyl side chain. The value for PS is indicated by the vertical arrow. The inset represents the difference $(\delta_{PS} - \delta_{PAMA})^2$ for each of the methacrylates.

Table 4. Equation of State Parameters for the Various Homopolymers

	T^* (K)	P^* (MPa)	ρ^* (g/cm^3)
PS	759	373	1.103
PMMA	644	500	1.270
PEMA	636	470	1.225
PPMA	628	440	1.171
PBMA	621	411	1.131
PHMA	606	351	1.028
POMA	591	292	0.945
PLMA	560	173	0.760

inset of Figure 9), while the results presented earlier suggest PS/PPMA is the most compatible system. However, the low accuracy of experimental values of δ, as well as the strong sensitivity of calculated values to the particular formalism chosen, complicate the use of this analysis as a quantitative predictive tool. Nevertheless, the success of the analysis presented here at capturing the main thermodynamic trends for this family of materials is encouraging. In fact, solubility parameters, having units of (energy/volume)$^{1/2}$, reflect a linkage between packing and energetics which is also apparent in densities or specific volumes. Therefore, comparison of the styrene and *n*-alkyl methacrylate homopolymer densities might shed additional light on the observed trend in phase behavior across the homologous copolymer series.

To this end, the Sanchez-Lacombe lattice fluid model was used to calculate the specific volume v_{spec} as a function of temperature. Specific volume was chosen rather than segmental volume, because the former is normalized with respect to the repeating unit molecular weight, thereby reflecting better the degree of cohesion expected for a given chemistry. The lattice fluid equation of state in the long chain limit is given as[13]

$$\tilde{P} + \tilde{\rho}^2 + \tilde{T}[\ln(1 - \tilde{\rho}) + \tilde{\rho}] = 0 \tag{5}$$

where $\tilde{P}$, $\tilde{\rho}$ and $\tilde{T}$ are the reduced pressure (P/P^*), density (ρ/ρ^*), and temperature (T/T^*). Equation 6 was solved for each homopolymer for temperatures ranging from 100 to 200 °C. The equation of state parameters ρ^*, T^*, and P^*, listed in Table 4, were calculated for each homopolymer using the group contributions listed in ref 40. Comparison with experimental *PVT* data was used,

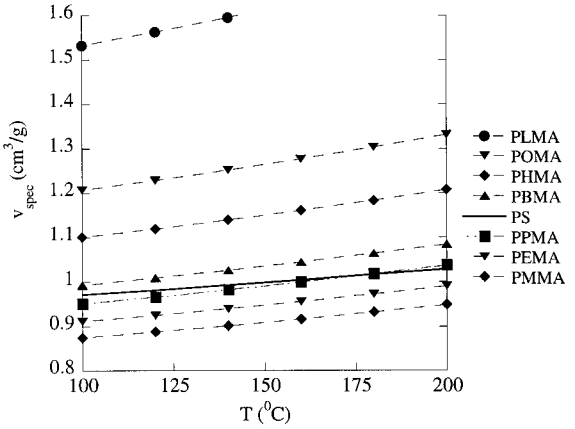

Figure 10. Calculated specific volumes of the different poly *n*-alkyl methacrylates and PS as a function of temperature.

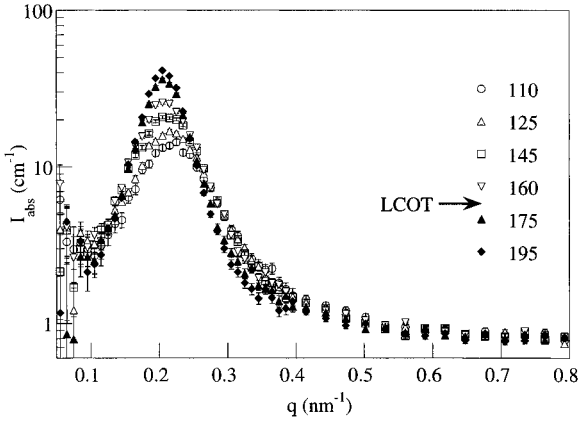

Figure 11. Scattering intensity profile for 80K PS-*b*-P(MMA-*r*-LMA).

whenever possible, to test the accuracy of these calculations. Excellent agreement was found for PS, PMMA, and PBMA for which extensive data is available in the literature.[41,42] The advantage of this analysis compared to the solubility parameter analysis presented above is its higher degree of accuracy, independent of the particular model used.[43]

Figure 10 represents the calculated v_{spec} for each homopolymer as a function of temperature. Again, it is seen that as the side chain length is increased from $n = 1$ to $n = 12$, the specific volume progresses from below (PMMA) to greatly above (PLMA) the values obtained for PS, while a close match is found for PPMA over the whole temperature range. The similarity between the curves obtained for PS and PPMA is striking, although a distinct difference in slope, and therefore in the thermal expansion coefficients of the two components, is apparent. This testifies to differences in self-interaction energy and packing efficiency for each of the components, although their resulting densities are very similar. Such differences are ultimately the origin of the LCOT behavior in this system.

For copolymers with longer alkyl side chains, the loss of thermodynamic compatibility can be ascribed to the following two effects. First, the magnitude of $\Delta\epsilon$ increases with increasing number of hydrocarbons in the alkyl side chain for $n \geq 6$, as indicated by the calculated solubility parameters. This is further suggested upon comparing the temperature-dependent portion of the fitted χ parameters for PS/PHMA, PS/POMA and PS/PLMA. Additionally, the "entropic" contributions to χ increase with increasing side chain length. The group contribution calculations of v_{spec} and δ support a picture of increasing asymmetry in both monomer structure and self-interaction energy that could explain this trend.

IV. Molecular Design of a New LCOT System. The success of the group contribution calculations in capturing the general trends in phase behavior for this family of materials prompted us to test their predictive capability. To this end, we sought to design a new styrene−methacrylate block copolymer that would exhibit the LCOT, using two methacrylate components that are individually immiscible with PS, namely, PMMA and PLMA. The composition of the random methacrylate block, denoted P(MMA-*r*-LMA), was selected by matching its specific volume and solubility parameter to that of polystyrene based on group contribution/equation-of-state calculations. In keeping with the intrinsic additivity assumption of group contribution models, the random copolymer sequence distribution was neglected. A close match in δ and v_{spec}, i.e., within the bounds of EMA to BMA, can be obtained for compositions ranging from 92 to 73 mol % methyl methacrylate (from 82 to 51.5 wt %). For our study, a composition of 74 mol % MMA (53 wt %) was chosen, yielding a δ of 18.16 $(J/cm^3)^{1/2}$ and a v_{spec} at 120 °C of 1.0021 cm^3/g. The resulting random copolymer block is expected to have similar properties to PBMA. Note that the same composition serves to match both δ and v_{spec}.

SANS profiles obtained for 80K PS-*b*-P(MMA-*r*-LMA) are shown in Figure 11. Clearly, this material is in the disordered state for temperatures below 160 °C, as evidenced by the broad scattering maximum around $q = 0.022$ Å^{-1}. Between 160 and 175 °C, the peak intensifies and sharpens, indicating the onset of order. This coincides remarkably well with 85K PS_{d8}-*b*-PBMA which orders at 165 °C.

The contrast between the phase behavior of this new material and that of both PS-*b*-PMMA and PS-*b*-PLMA, which only exhibit the UCOT, is indisputable. It demonstrates how LCOT behavior can be imparted to block copolymers by preparing the first block as a random copolymer of two components otherwise immiscible with the second block, making a judicious choice in composition. A similar mechanism of mixing leads to the widely known compatibilization of polystyrene and poly(methyl methacrylate) through the copolymerization of styrene with acrylonitrile.[44] More generally, the success of this molecular design exercise suggests a simple, semiquantitative approach to designing the phase behavior of blends and copolymers, at least for weakly interacting systems.

Conclusion

Investigation of the phase behavior of a family of diblock copolymers between styrene and a homologous series of *n*-alkyl methacrylates has revealed that two markedly different phase behaviors are seen for these materials, depending on the alkyl side chain length. For alkyl side chains containing six or more hydrocarbons, UCOT phase behavior similar to that of PS-*b*-PMMA is observed, with a weakly temperature-dependent χ. For shorter alkyl side chains, however, the observed phase behavior is similar to that reported for PS-*b*-PBMA, namely, some miscibility at low temperatures and ordering of the two blocks at elevated temperatures. A

maximum in thermodynamic compatibility was found for PS-*b*-PPMA.

These observations are supported by combined group contribution/equation of state model calculations of the solubility parameter and specific volume of the corresponding homopolymers. The calculations show that δ and v_{spec} of polystyrene are best matched around propyl and butyl methacrylate, which favors miscibility at low temperatures for the corresponding copolymers. The compatibility found for these systems is, however, still rather marginal compared to strongly polar systems such as PMMA/PEO, which explains why their LCOTs lie in an experimentally accessible temperature range for intermediate molecular weights (~100 000).

We further showed how these simple calculations could successfully be used to design-in low temperature miscibility and a LCOT into the phase diagram of a new diblock copolymer of styrene and a random copolymer of methyl and lauryl methacrylate. The success of this approach suggests a simple semiquantitative method for predicting and designing the phase behavior of weakly interacting polymer pairs.

Acknowledgment. This work was supported in part by the National Science Foundation under Award No. DMR-9357682 (A.M.M.), and by the DOE BES under Award No. DE FG02 96ER45 (T.P.R.) and the MRSEC program of the National Science Foundation under Award No. DMR-9400488 (T.P.R.). This material is based upon activities supported by the National Science Foundation under Agreement No. DMR-9423101. A.-V.G.R. acknowledges the partial support of the Belgian and American Educational Foundation.

References and Notes

(1) Leibler, L. *Macromolecules* **1980**, *13*, 1602.
(2) Fredrickson, G. H.; Helfand, E. *J. Chem. Phys.* **1987**, *87*, 697.
(3) Fredrickson, G. H.; Helfand. E. *J. Chem. Phys.* **1988**, *89*, 5890.
(4) Bates, F. S. *Macromolecules* **1984**, *17*, 2607.
(5) Rosedale, J. H.; Bates, F. S. *Macromolecules* **1990**, *23*, 2329.
(6) Almdal, K.; Rosedale, J. H.; Bates, F. S. *Macromolecules* **1990**, *23*, 4336.
(7) Bates, F. S.; Rosedale, J. H.; Fredrickson, G. H. *J. Chem. Phys.* **1990**, *92*, 6255.
(8) Rosedale, J. H.; Bates, F. S.; Almdal, K.; Mortensen, K.; Wignall, G. D. *Macromolecules* **1995**, *28*, 1429.
(9) Winey, K. I.; Gobran, D. A.; Xu, Z.; Fetters, L. J.; Thomas, E. L. *Macromolecules* **1994**, *27*, 2392.
(10) Russell, T. P.; Karis, T. E.; Gallot, Y.; Mayes, A. M. *Nature* **1994**, *368*, 729.
(11) Karis, T. E.; Russell, T. P.; Gallot, Y.; Mayes, A. M. *Macromolecules* **1995**, *28*, 1129.
(12) Hashimoto, T.; Hasegawa, H.; Hashimoto, T.; Katayama, H.; Kamigaito, M.; Sawamoto, M.; Imai, M. *Macromolecules* **1997**, *30*, 6819.
(13) Sanchez, I. C.; Panayiotou, C. G. *Models for Thermodynamic and Phase Equilibria Calculations*; Marcel Dekker: New York, 1994; p 187.
(14) Janssen, S.; Schawhn, D.; Mortensen, K.; Springer, T. *Macromolecules* **1993**, *26*, 5587.
(15) Hammouda, B.; Bauer, B. J. *Macromolecules* **1995**, *28*, 4505.
(16) Pollard, M.; Russell, T. P.; Ruzette, A.-V. G.; Mayes, A. M.; Gallot, Y. *Macromolecules* **1998**, *31*, 6493.
(17) Dudowicz, J.; Freed, K. F. *J. Chem. Phys.* **1992**, *96*, 9147.
(18) Bidkar, U. R.; Sanchez, I. C. *Macromolecules* **1995**, *28*, 3963.
(19) Dudowicz, J.; Freed, K. F. *Macromolecules* **1993**, *26*, 213.
(20) Yeung, C.; Desai, R. C.; Shi, A.-C.; Noolandi, J. *Phys. Rev. Lett.* **1994**, *72*, 1834.
(21) Hino, T.; Prausnitz, J. M. *Macromolecules* **1998**, *31*, 2636.
(22) Bernstein, R. E.; Cruz, C. A., Paul, D. R., Barlow, J. W. *Macromolecules* **1977**, *10*, 681.
(23) Cortazar, M.; Calahorra, E.; Guzman, G. M. *Eur. Polym. J.* **1981**, *19*, 1925.
(24) Nishi, T.; Kwei, T. K. *Polymer* **1975**, *16*, 285.
(25) McMaster, L. P. *Macromolecules* **1973**, *6*, 760.
(26) Hammouda, B.; Bauer, B. J.; Russell, T. P. *Macromolecules* **1994**, *27*, 2357.
(27) Russell, T. P.; Hjelm, R. P.; Seeger, P. A. *Macromolecules* **1990**, *23*, 890.
(28) Stühn, B. *J. Polym. Sci., Polym. Phys. Ed.* **1992**, *30*, 1013.
(29) Allen, R. D.; Long, T. E.; McGrath, J. E. *Polym. Bull.* **1986**, *15*, 127.
(30) Freed, K. F.; Dudowicz, J. *J. Chem. Phys.* **1992**, *97*, 2105.
(31) Freed, K. F.; Dudowicz, J. *Macromolecules* **1996**, *29*, 625.
(32) Foreman, K. W.; Freed, K. F. *J. Chem. Phys.* **1997**, *106*, 7422.
(33) Schweizer, K. S. *Macromolecules* **1993**, *26*, 6050.
(34) Kumar, S. K. *Macromolecules* **1997**, *30*, 5085.
(35) Harris, D. G. Synthesis and Characterization of Poly(styrene-*b*-*n*-butyl methacrylate). S.B. Thesis, Massachusetts Institute of Technology, 1998; p 28.
(36) Brannock, G. R.; Barlow, J. W.; Paul, D. R. *J. Polym. Sci., Polym. Phys. Ed.* **1991**, *29*, 413.
(37) Hildebrand, J. H.; Scott, R. L. *The Solubility of Non-Electrolytes*, 3rd ed.; Reinhold: New York, 1959.
(38) Van Krevelen, D. W.; Hoftyzer, P. J. *Properties of Polymers. Correlations with Chemical Structure*; Elsevier: New York, 1972.
(39) Rogers, S. S.; Mandelkern, L. *J. Chem. Phys.* **1957**, *61*, 985.
(40) Boudouris, D.; Constantinou, L.; Panayiotou, C. *Ind. Eng. Chem. Res.* **1997**, *36*, 3968.
(41) Quach, A.; Simha, R. *J. Appl. Phys.* **1971**, *41*, 4592.
(42) Olabisi, O.; Simha, R. *Macromolecules* **1975**, *8*, 206.
(43) Rodgers, P. A. *J. Appl. Polym. Sci.* **1993**, *48*, 1061.
(44) Fowler, M. E.; Barlow, J. W.; Paul, D. R. *Polymer* **1987**, *28*, 1177.

MA981055C